Am J Physiol Endocrinol Metab 305: E367–E375, 2013.
First published June 4, 2013; doi:10.1152/ajpendo.00644.2012.

Interactions between p-Akt and Smad3 in injured muscles initiate myogenesis or fibrogenesis

Yanjun Dong,[1,3] Ronak Lakhia,[1] Sandhya S. Thomas,[1] Yanlan Dong,[1] Xiaonan H. Wang,[2] Kleiton Augusto Santos Silva,[1,4] and Liping Zhang[1]

[1]*Nephrology Division, Department of Medicine, Baylor College of Medicine, Houston, Texas;* [2]*Renal Division, Department of Medicine, Emory University, Atlanta, Georgia;* [3]*Beijing An Zhen Hospital Affiliated to Capital Medical University, Beijing Institute of Heart, Lung, and Blood Vessel Diseases, Beijing, China; and* [4]*Nephrology Division, Department of Medicine, Federal University of São Paulo, São Paulo, Brazil*

Submitted 20 December 2012; accepted in final form 28 May 2013

Dong Y, Lakhia R, Thomas SS, Dong Y, Wang XH, Silva KA, Zhang L. Interactions between p-Akt and Smad3 in injured muscles initiate myogenesis or fibrogenesis. *Am J Physiol Endocrinol Metab* 305: E367–E375, 2013. First published June 4, 2013; doi:10.1152/ajpendo.00644.2012.—In catabolic conditions such as aging and diabetes, IGF signaling is impaired and fibrosis develops in skeletal muscles. To examine whether impaired IGF signaling initiates muscle fibrosis, we generated IGF-IR$^{+/-}$ heterozygous mice by crossing loxP-floxed IGF-IR (exon 3) mice with MyoD-cre mice. IGF-IR$^{+/-}$ mice were studied because we were unable to obtain homozygous IGF-IR-KO mice. In IGF-IR$^{+/-}$ mice, both growth and expression of myogenic genes (MyoD and myogenin; markers of satellite cell proliferation and differentiation, respectively) were depressed. Likewise, in injured muscles of IGF-IR$^{+/-}$ mice, there was impaired regeneration, depressed expression of MyoD and myogenin, and increased expression of TGF-β1, α-SMA, collagen I, and fibrosis. To uncover mechanisms stimulating fibrosis, we isolated satellite cells from muscles of IGF-IR$^{+/-}$ mice and found reduced proliferation and differentiation plus increased TGF-β1 production. In C_2C_{12} myoblasts (a model of satellite cells), IGF-I treatment inhibited TGF-β1-stimulated Smad3 phosphorylation, its nuclear translocation, and expression of fibronectin. Using immunoprecipitation assay, we found an interaction between p-Akt or Akt with Smad3 in wild-type mouse muscles and in C_2C_{12} myoblasts; importantly, IGF-I increased p-Akt and Smad3 interaction, whereas TGF-β1 decreased it. Therefore, in muscles of IGF-IR$^{+/-}$ mice, the reduction in IGF-IR reduces p-Akt, allowing for dissociation and nuclear translocation of Smad3 to enhance the TGF-β1 signaling pathway, leading to fibrosis. Thus, strategies to improve IGF signaling could prevent fibrosis in catabolic conditions with impaired IGF signaling.

transforming growth factor-β1; insulin-like growth factor I; satellite cells; myogenesis; fibrosis; Smad3

SATELLITE CELLS REPRESENT A DISTINCT LINEAGE of myogenic progenitor cells that are responsible for postnatal growth, repair, and maintenance of skeletal muscle (34). Normally, satellite cells are quiescent in adult muscle, but following muscle injury they are converted into myoblasts that proliferate and migrate to the site of injury to differentiate and form new myofibers (15).

Growth factors influence the processes of satellite cell activation and muscle regeneration in injured muscles of rodents. Of these, the most extensively studied are hepatocyte growth factor (24), basic fibroblast growth factor (2), insulin-like growth factor I (IGF-I) and IGF-II, transforming growth factor-β (TGF-β), and others. For example, hepatocyte growth factor can promote quiescent satellite cells to enter the cell cycle to stimulate muscle regeneration (24); local expression of a muscle-specific IGF-I transgene increases satellite cell function to accelerate muscle regeneration (3, 11, 25, 27). In vitro, TGF-β can depress satellite cell proliferation and differentiation in a dose-dependent manner (1). TGF-β1 also induces transdifferentiation of satellite cells into myofibroblasts that produce fibrosis and hinder regeneration of injured muscles (20). In contrast, suppression of TGF-β1 signaling inhibits fibrosis and improves muscle regeneration (23). However, whether growth factors and their signaling pathway interact to regulate satellite cell function and muscle regeneration is unclear.

In muscles of animal models of aging, diabetes, or chronic kidney disease (CKD), IGF/insulin intracellular signaling is impaired, fibrous tissue is accumulated, and muscle regeneration is decreased following injury (4, 7, 12, 13, 17). For example, in injured muscles of mice with CKD, we found that decreased function of IGF-I leads to satellite cell dysfunction, decreased muscle regeneration, and an increase in muscle fibrosis (46). However, the mechanism(s) by which impaired IGF signaling causes fibrosis is unclear. Because of fibrotic responses to TGF-β1, we proposed that impaired IGF signaling would promote fibrosis through a TGF-β1-based mechanism. To evaluate this hypothesis, we created mice that were heterozygous IGF-IR-knockout mice, but only in MyoD-expressing cells. These transgenic mice had impaired muscle growth, and their satellite cells exhibited decreased myogenesis and increased fibrogenesis. Our results identify an interaction between p-Akt and Smad3 that may be modulating fibrosis in skeletal muscles of conditions with impaired IGF signaling.

MATERIALS AND METHODS

Reagent and antibodies. Antibodies against p-Akt (Ser^{473}), p-Smad3 (Ser$^{423/425}$), and Smad3 were from Cell Signaling Technology (Beverly, MA). Antibodies against IGF-IR and TGF-β1 were from Santa Cruz Biotechnology (Santa Cruz, CA), against MyoD from Vector Laboratories (Burlingame, CA), and against eMyHC and myogenin from the Developmental Studies Hybridoma Bank (University Iowa, Iowa City, IA). Cardiotoxin, Sirius red, and antibodies of anti-laminin, anti-α-smooth muscle actin (α-SMA), and anti-fibronectin were from Sigma-Aldrich (St. Louis, MO). The anti-Ki67-Alexa Fluor 555 antibody was from BD Bioscience (San Jose, CA), whereas DMEM and FBS were from Cellgro Mediatech (Manassas, VA).

Address for reprint requests and other correspondence: L. Zhang, Baylor College of Medicine, Nephrology Division, M/S, BCM 395, One Baylor Plaza, ABBR R705, Houston, TX 77030 (e-mail: lipingz@bcm.edu).

Generation of mice lacking IGF-IR in MyoD-expressing cells. Animal protocols were approved by the Baylor College of Medicine Institutional Animal Care and Use Committees. Transgenic mice bearing MyoD-Cre were a gift from Dr. D. J. Goldhamer (University of Connecticut, Storrs, CT) (5). Mice with loxp-floxed IGF-IR (IGF-IR$^{flox/flox}$) were bred with MyoD-Cre mice (16). Mice with MyoD-Cre and loxP-floxed IGF-IR were identified by genotyping (Cre primer: 5′-TGCCTGCATTACCGGTCGATG-3′ and 5′-CCATGAGTGA-ACGAACCTGGTCG-3′; IGF-IR-loxp primer: P1, 5′-CGCCTG-GAAAAC TGCACG-3′; P2: 5′-AGCTGCCCAGGCACTCCG-3′; P3: 5′-GCAGGGGATACAGTACATGTTT-3′). RT-PCR produces 518 bp (i.e., P1–P3) corresponding to IGF-IR exon 3 knockout, where the 574-bp fragment indicated the intact IGF-IR gene (6, 16) (Fig. 1*A*). We were unable to obtain homozygous IGF-IR-knockout mice, so we studied heterozygous IGF-IR$^{flox/-}$/MyoD-Cre mice (refered as IGF-IR$^{+/-}$).

Muscle regeneration. IGF-IR$^{+/-}$ and control (IGF-IR$^{flox/flox}$) mice were studied at 6–10 wk of age. Muscle injury is induced by cardiotoxin (CTX) injection to activate satellite cells and muscle regeneration because CTX induces myofiber degeneration but does not affect satellite cells, blood vessels, or muscle innervation (9). Briefly, 80 μl of 10 μM CTX in saline was injected into one tibialis anterior (TA) muscle of anesthetized mice, using a 27-gauge needle. The contralateral muscle was injected with same volume of PBS and served as an uninjured control muscle. After different periods, mice were anesthetized and perfused with PBS via puncture of the left ventricle. Muscles were either frozen in isopentane chilled with dry ice for histological analyses or frozen and stored at −80°C until proteins or RNAs were evaluated.

Satellite cell isolation. Satellite cells were isolated from 2-wk-old young mice and identified by previously described methods (46). Satellite cell proliferation was assessed using a percentage of Ki-67-positive nuclei to total nuclei. TGF-β1 in medium from cultured satellite cells was analyzed by ELISA (Promega, Madison, WI).

Differentiation assays. C_2C_{12} cells (ATCC, Manassas, VA) or isolated satellite cells were differentiated into myotubes as described (42). Myotubes were fixed in 2% paraformaldehyde for 10 min before immunostaining for embryonic myosin heavy chain (eMyHC). The differentiation index was calculated as the percentage of nuclei within

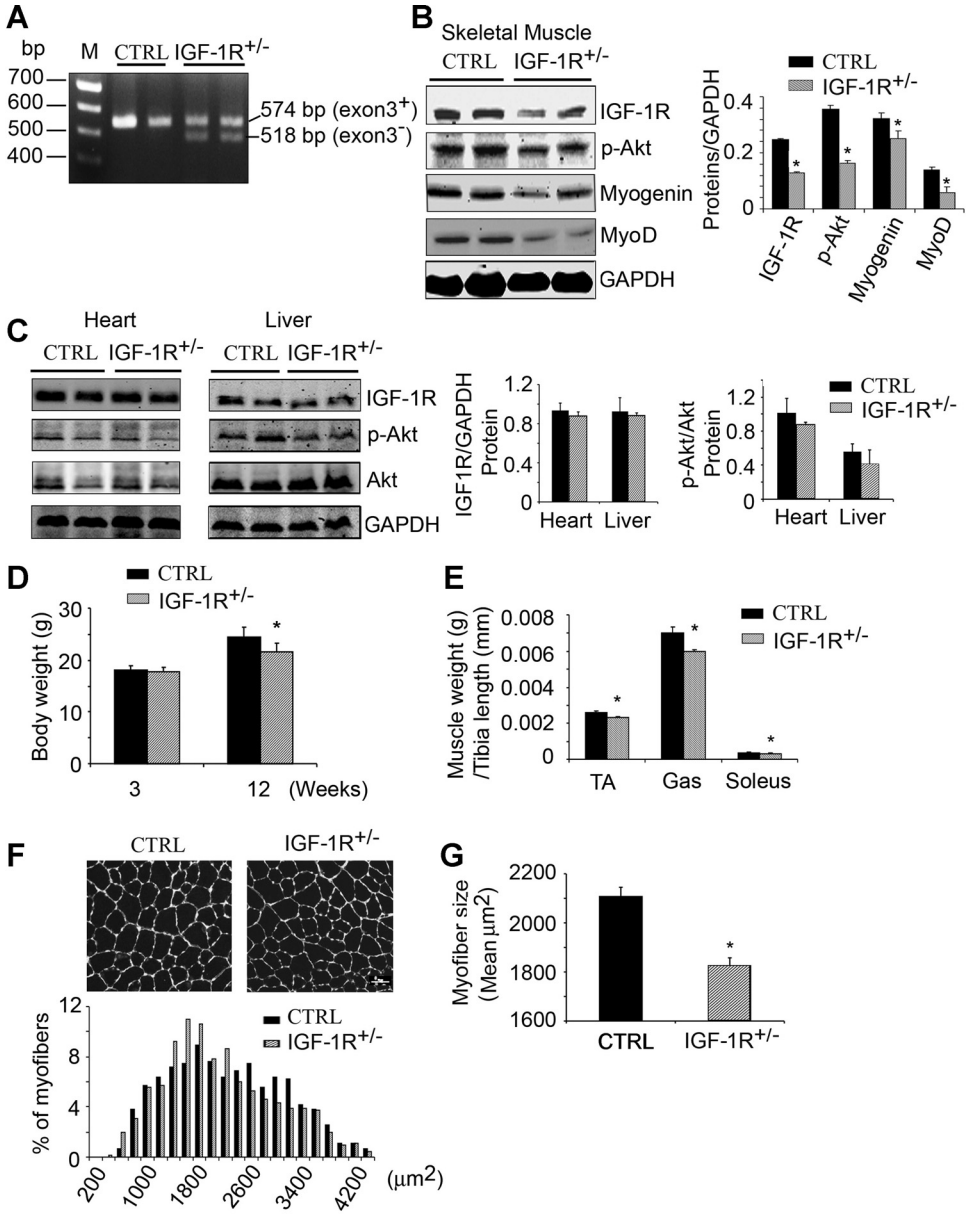

Fig. 1. IGF-IR$^{+/-}$ impairs IGF-I signaling in mouse muscle and decreases muscle growth. *A*: genomic analysis (PCR) confirms deletion of exon 3 of the IGF-IR in IGF-IR$^{+/-}$ mice ($n = 6$ mice in each group). *B*: representative Western blots of the indicated proteins in muscles of control (CTRL; IGF-IR$^{lox/lox}$) or IGF-IR$^{+/-}$ mice (*left*). Band densities corrected for GAPDH are on the *right* ($n = 4$ mice in each group). *C*: representative Western blots of the indicated proteins in heart and liver of CTRL or IGF-IR$^{+/-}$ mice (*left*). Band densities corrected for GAPDH or Akt are on the *right* ($n = 4$ mice in each group). *D*: body weights of CTRL and IGF-IR$^{+/-}$ mice at 3 and 12 wk after birth ($n = 5$ mice in each group). *E*: ratios of muscle weight to tibia length in CTRL or IGF-IR$^{+/-}$ mice at 12 wk of age (soleus, soleus muscle; TA, tibialis anterior; gas, gastrocnemius; $n = 5$ mice in each group). *F*, *top*: cross-sections of TA muscles were immunostained with anti-laminin (bar, 50 μm); *bottom*: myofiber areas were used to determine the percentage of myofibers in a defined area to total no. of myofibers measured (total of 500 myofibers were measured from each group of 4 mice). *G*: the mean ± SE size of myofibers found in *F*; $n = 4$ mice in each group. *$P <$ 0.05 vs. CTRL.

myotubes that was positively stained for eMyHC plus the number of eMyHC positive-mononuclear cells to the total number of nuclei in the area (43). In striated muscles there are multiple forms of myosin heavy chains encoded by different genes, producing tissue-specific and developmentally regulated expression. We studied eMyHC protein representing embryonic myosin heavy chain, which is progressively lost during postnatal development. Notably, eMyHC is expressed during muscle regeneration. The individual counting the fibers was masked to treatment or physiological conditions.

RT-PCR analysis. RT-PCR was performed as described (45, 46), and relative gene expression was calculated from cycle threshold (C_T)values using GAPDH as an internal control [relative expression = $2^{(\text{sample } C_T - \text{GAPDH } C_T)}$]. Primer sequences have been reported (44).

Immunohistochemical analyses. Serial, transverse cryosections (8 μm) of TA muscles were air-dried and fixed in cold acetone or 4% paraformaldehyde for 10 min. They were stained with hematoxylin and eosin (H & E); other sections were examined for collagen and fibrosis using Sirius red staining (46).

To calculate cross-sectional areas of individual myofibers, cross-sections of TA muscles were immunostained with anti-laminin to identify the basement membrane. Myofiber sizes were measured using Nikon NIS-Elements Br 3.0 software (Melville, NY), and the myofiber sizes were expressed as the percentage of myofibers within the specified range. The individual counting the myofibers was masked to treatment and physiological conditions.

Immunoprecipitation assay. Lysates of gastrocnemius muscles (1 mg) from wild-type mice were incubated with anti-Akt or anti-p-Akt conjugated to sepharose beads and shaken overnight at 4°C. The beads were washed five times with PBS, and Western blots were performed using anti-Smad3 or p-Smad3. Alternatively, the lysate was immunoprecipitated with anti-Smad3 or anti-p-Smad3 overnight at 4°C. After the addition of 30 μl of Protein A/G Plus beads for 2 h at 4°C, the beads were washed five times with PBS, and Western blots were performed using anti-Akt or p-Akt. C_2C_{12} myoblasts were treated with IGF-I (10 ng/ml), TGF-β1 (4 ng/ml), or both for 30 min. Cell lysates (500 μg) were immunoprecipitated using methods and antibodies as described above.

Statistical analysis. Results are expressed as means ± SE. Significance testing was performed using one-way ANOVA, followed by pairwise comparisons using the Student-Newman-Keuls test. Statistical significance was set at $P < 0.05$. A minimum of three replicates was performed for each experimental condition.

RESULTS

Mice with IGF-IR$^{+/-}$ impair IGF signaling in mouse muscle and decrease muscle growth. Using the strategy described before (6, 16), we confirmed that IGF-IR$^{+/-}$ mice had deletion of exon 3 (Fig. 1*A*). In muscles of these mice, the IGF-IR protein was ~50% lower than in muscles of control IGF-IR$^{flox/flox}$ mice (Fig. 1*B*). In lysates of muscles from IGF-IR$^{+/-}$ mice, the levels of p-Akt, MyoD, and myogenin were also lower vs. the results from control mice (Fig. 1*B*). To test whether IGF-IR$^{+/-}$ affected the other tissues, we assessed the hearts and livers of control and IGF-IR$^{+/-}$ mice. We found no significant differences in the levels of IGF-IR or p-Akt in the hearts or livers of control or IGF-IR$^{+/-}$ mice, although there was a slight reduction of protein in IGF-IR$^{+/-}$ mice (Fig. 1*C*). Thus, the major response of IGF-IR knockout in MyoD-expressing cells occured in skeletal muscles. At 3 wk of age, body weights of IGF-IR$^{+/-}$ and control mice were not significantly different, but at 12 wk of ag, the weight of IGF-IR$^{+/-}$ mice was significantly lower than that of control mice (Fig. 1*D*). In IGF-IR$^{+/-}$ mice, the ratio of muscle weight to tibia length was significantly lower than in control mice (Fig. 1*E*). Mixed-fiber TA and gastrocnemius muscles were decreased by 10.34 ± 1.5 and 14.81 ± 3.08%, respectively, compared with values in control mice, whereas the decrease in the red fiber soleus muscle was 12.33 ± 2.97%. However, the magnitude decrease in weight among the three different types of muscles was not significantly different. Therefore, different types of muscle fibers are equally affected in IGF-IR$^{+/-}$ mice. Next, we measured sizes of myofibers in TA muscles from IGF-IR$^{+/-}$ and wild-type mice. The distribution of myofiber sizes in IGF-IR$^{+/-}$ vs. control mice was shifted to the left, with an average size of 1,959.88 ± 32.1 (in IGF-IR$^{+/-}$ mice) vs. 2,145.1 ± 36.1 μm^2 (control mice) ($P < 0.05$; Fig. 1, *F* and *G*).

Mice with IGF-IR$^{+/-}$ had decreased satellite cell function. We isolated satellite cells from muscles of IGF-IR$^{+/-}$ and control mice. These cells had significantly reduced expression of IGF-IR and p-Akt as well as MyoD and myogenin (Fig. 2*A*), which are markers of satellite cell proliferation and differentiation, respectively. In satellite cells from muscles of IGF-IR$^{+/-}$ mice there was decreased proliferation, as assesed by Ki-67 immunostaining (Fig. 2*B*). There was also impaired differentiation as evaluated by immunostaining for embryonic myosin heavy chain, which is expressed in muscle regeneration (eMyHC; Fig. 2*C*). In isolated satellite cells from muscles of IGF-IR$^{+/-}$ mice, there was increased fibronectin expression plus production of 50% more TGF-β1 vs. values from satellite cells isolated from control mice (Fig. 2, *D* and *E*). Therefore, impaired IGF signaling in satellite cells decreases their proliferation and differentiation into myotubes while stimulating TGF-β1 production and markers of fibrosis.

IGF-IR$^{+/-}$ impairs muscle regeneration. Next, we used CTX-induced muscle injury to examine satellite cell activation in vivo (27, 46). At 3 days after injury, the mRNA levels of myogenic genes, MyoD, and myogenin were maximal in muscles of both groups of mice (Fig. 3, *A* and *B*). But at 2, 3, or 11 days after injury, both MyoD and myogenin mRNAs were significantly lower in muscles of IGF-IR$^{+/-}$ mice. By 14 days, the mRNAs in both groups had returned to preinjury levels.

H & E staining of cross-sections of injured TA muscles revealed slowed muscle regeneration in IGF-IR$^{+/-}$ mice. At 5 or 7 days after injury, muscles from IGF-IR$^{+/-}$ mice had fewer newly formed myofibers, as indicated by central nuclei (Fig. 3, *C* and *D*), and at 14 days after injury, space between myofibers persisted (Fig. 3*C*), and the distribution of newly formed myofiber sizes was shifted toward smaller sizes, with an average size of 1,147.5 ± 20.8 vs. 1,417.2 ± 26.0 μm^2 ($P < 0.05$; Fig. 3, *E* and *F*). Thus, reduced IGF signaling impairs satellite cell function in vivo to decrease muscle regeneration.

Muscle injury stimulates fibrosis in muscle of IGF-IR$^{+/-}$ mice. Muscle injury increased IGF-IR expression in muscle of control mice but not in muscle of IGF-IR$^{+/-}$ mice (Fig. 4*A*). In injured muscle of IGF-IR$^{+/-}$ mice, there was increased TGF-β1 mRNA and protein expression (Fig. 4, *B* and *C*). Specifically, there was evidence for increased TGF-β1 signaling, as p-Smad3 was increased in injured muscles of IGF-IR$^{+/-}$ mice (Fig. 4*C*). These results are consistent with an increase in protein and mRNAs of α-SMA (Fig. 4, *C* and *D*) and mRNA of collagen I (Fig. 4*E*) as well as accumula-

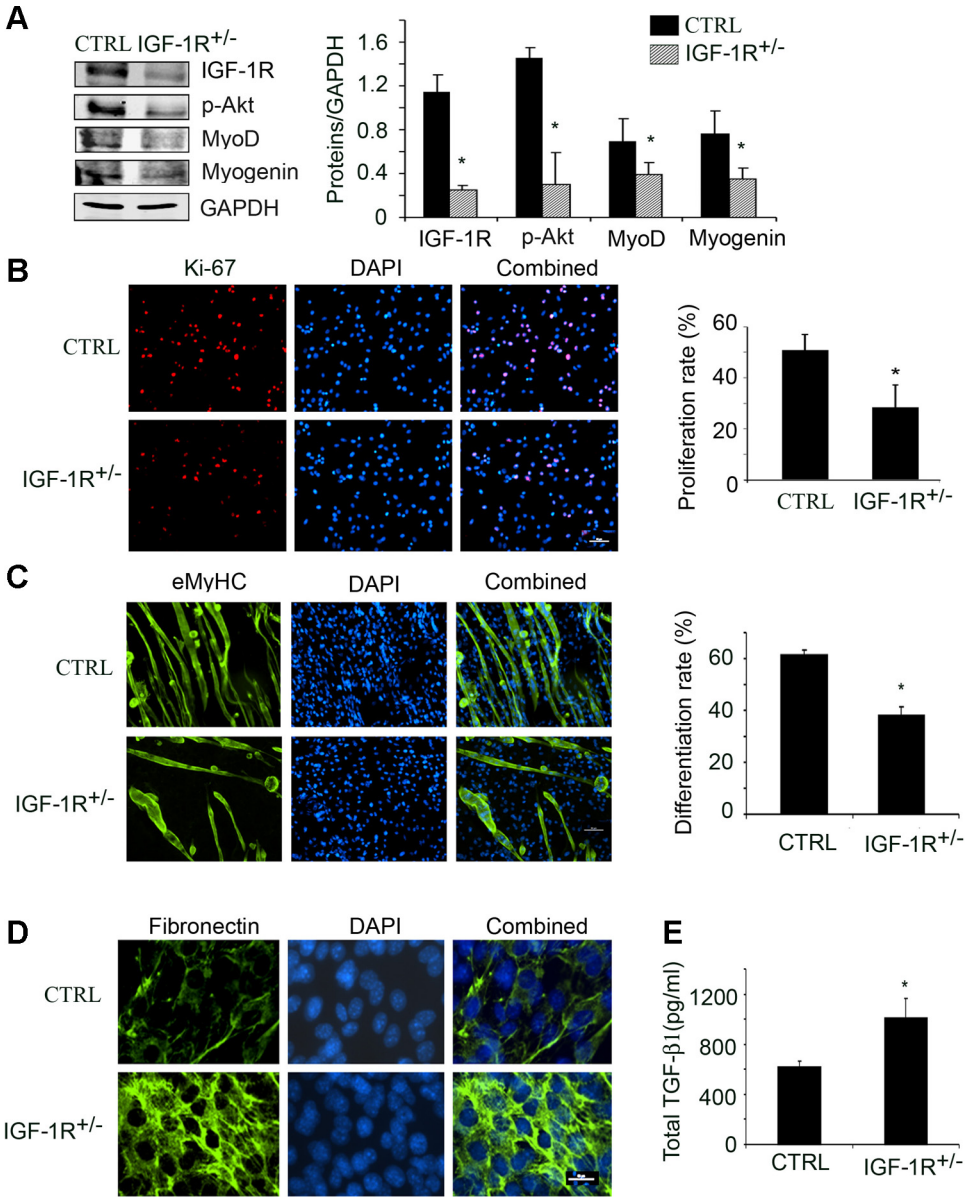

Fig. 2. IGF-IR$^{+/-}$ decreases satellite cell functions. *A*, *left*: representative Western blots of the indicated proteins in satellite cells isolated from muscles of CTRL or IGF-IR$^{+/-}$ mice; *right*: band densities (n = 3 mice in each group). *B*: the percentage of Ki-67-positive cells to total satellite cells was calculated to identify a proliferation rate (bar, 50 μm; satellite cells were isolated from 3 mice, and the experiments were repeated 3 times). *C*, *left*: differentiated satellite cells were immunostained with an antibody against embryonic myosin heavy chain (eMyHC; green); *right*: the differentiation index was calculated as described in MATERIALS AND METHODS. (bar, 50 μm; satellite cells were isolated from 2 mice, and the experiments were repeated 3 times). *D*: satellite cells were immunostained for fibronectin (green; bar, 50 μm). Two mice in each group were used to isolate satellite cells, and the experiments were repeated 3 times. *E*: total transforming growth factor-β1 (TGF-β1) was measured in media from incubated satellite cells of control or IGF-IR$^{+/-}$ mice (n = 3 mice in each group, and the measurements were repeated 3 times). *$P < 0.05$ vs. CTRL.

tion of collagen (Sirius red staining; Fig. 4*F*) following injury. However, in uninjured muscles of IGF-IR$^{+/-}$ mice, the protein levels of TGF-β1, collagen I, α-SMA, or p-Smad3 were not significantly changed vs. control mice (Fig. 4*G*). Therefore, in injured muscles of IGF-IR$^{+/-}$ mice, TGF-β1 increases and promotes fibrosis.

IGF-I inhibits TGF-β1-suppressed muscle cell differentiation and increased fibrosis. Next, we examined how a decrease in IGF-IR promotes fibrosis in injured muscles. We stimulated C_2C_{12} myoblasts by placing them in differentiation media with IGF-I (10 ng/ml), TGF-β1 (4 ng/ml), or both. After 96 h we found that TGF-β1 blunted C_2C_{12} differentiation into myotubes, whereas IGF-I blocked the responses to TGF-β1 (Fig. 5*A*). When C_2C_{12} myoblasts were treated with TGF-β1, IGF-I, or both for 8 h, TGF-β1 alone increased fibronectin expression, and IGF-I significantly inhibited this TGF-β1 response (Fig. 5, *B* and *C*).

The interaction of p-Akt with Smad3 blocks Smad3 nuclear translocation. To identify how reduced IGF-IR in MyoD-expressing cells leads to fibrosis following muscle injury, we treated C_2C_{12} myoblasts with IGF-I, TGF-β1, or both for 30 min. Western blots of cell lysates revealed that IGF-I raised p-Akt, whereas TGF-β1 increased the p-Smad3 level. But when IGF-I and TGF-β1 were combined, the p-Smad3 level was decreased vs. results in cells treated with TGF-β1 alone (Fig. 6*A*). To test whether the IGF-I-induced increase in p-Akt regulates Smad3 activation, we evaluated Smad3 nuclear translocation in C_2C_{12} myoblasts. TGF-β1 stimulated the nuclear translocation of Smad3, and the addition of IGF-I markedly suppressed it. In these cells, we also found that p-Akt colocalized with Smad3 in the cytoplasm of C_2C_{12} myoblasts (Fig. 6*B*). Thus, IGF-I signaling can suppress TGF-β1 signaling in myoblasts and prevent Smad3 translocation into the nucleus.

Next, we isolated satellite cells from muscles of IGF-IR$^{+/-}$ mice. Compared with satellite cells from control mice, satellite cells from muscle of IGF-IR$^{+/-}$ mice had lower levels of IGF-IR or p-Akt but increased Smad3 in the nuclei (Fig. 6*C*). We also noticed the nuclei staining of IGF-IR or p-Akt in

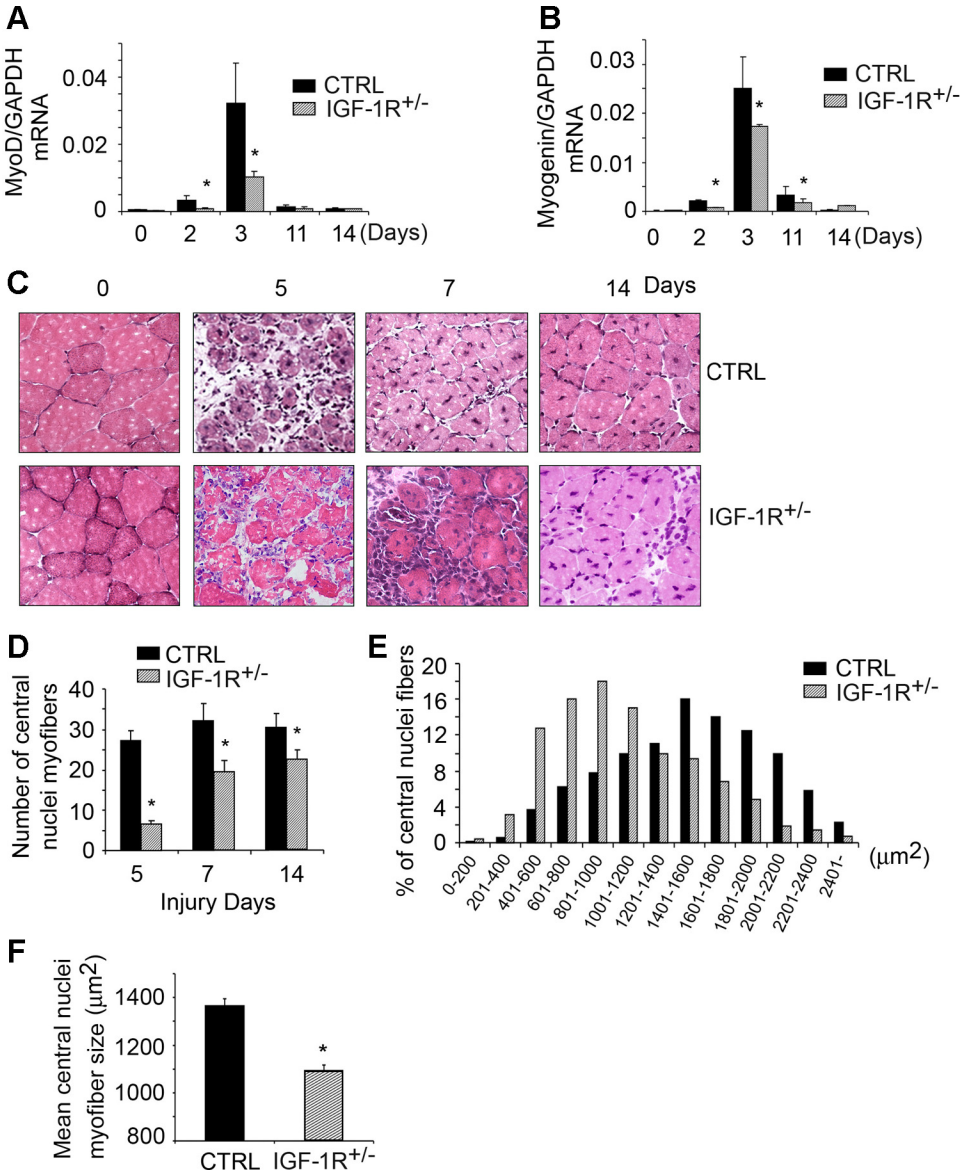

Fig. 3. IGF-IR$^{+/-}$ impairs muscle regeneration. In injured mouse muscle, mRNAs of MyoD (*A*) or myogenin (*B*) corrected for GAPDH were evaluated by RT-PCR ($n = 4$ mice at each time point). *C*: hematoxylin and eosin-stained cross-sections of TA muscles at 5, 7, and 14 days after injury (bar, 20 μm; 4 control or IGF-IR$^{+/-}$ mice at each time point were evaluated). *D*: average no. of myofibers from 5 areas in *C*, with central nuclei (i.e., newly formed myofibers) counted ($n = 4$ mice in each group). *E*: at 14 days after injury, the distribution of the cross-sectional areas of newly formed myofibers in TA muscles was calculated (a total of 700 new generated myofibers were measured from 4 wild-type CTRL or IGF-IR$^{+/-}$ mice). *F*: mean ± SE size of newly produced myofibers found in E; $n = 4$ mice in each group. *$P < 0.05$ vs. CTRL.

satellite cells of IGF-IR$^{+/-}$ mice, which could reflect from DAPI channel leakage upon extended exposure. There also was colocalization of p-Akt and Smad3 in satellite cells of control mice. These results provide in vivo evidence for a cross-talk between the IGF-I and TGF-β1 signaling.

From the results with muscle cells, we proposed that p-Akt sequesters Smad3 in the cytoplasm and suppresses TGF-β1 signaling (there is evidence from cancer cells that Akt associates with Smad3) (8, 28). To test our proposal, we immunoprecipitated muscle lysates with anti-Akt, anti-p-Akt, anti-Smad3, or anti-p-Smad3. Each immunocomplex was immunoblotted with anti-Smad3, anti-p-Smad3, anti-Akt, or anti-p-Akt. The results of these immunoprecipitation/Western blotting experiments indicate that both p-Akt and Akt associate with Smad3 but not p-Smad3 in muscles of wild-type mice (Fig. 6*D*). The major form of Akt interacting with Smad3 is p-Akt (Fig. 6*D*). Besides evaluating the proposal in mouse muscles, we treated C_2C_{12} myoblasts with IGF-I, TGF-β1, or both for 30 min. Cell lysates were immunoprecipitated with antibodies to Smad3, p-Smad3, Akt, or p-Akt, and their immunocomplexes were subjected to Western blot with the indicated proteins (Fig. 6*E*). Results from these experiments showed that Akt or p-Akt associates with Smad3 but not p-Smad3. However, IGF-I increased the association of Smad3 with p-Akt. In contrast, TGF-β treatment decreased the association of Smad3 with p-Akt (Fig. 6*E*).

DISCUSSION

Catabolic conditions of impaired IGF/insulin signaling (i.e., CKD, diabetes, or aging) lead to reduced satellite cell function and muscle regeneration and increased muscle fibrosis (46). However, how impaired IGF-I/insulin signaling leads to fibrosis has not been elucidated. In muscles from IGF-I$^{+/-}$ mice we found reduced levels of IGF-IR, p-Akt, MyoD, and myogenin, which lead to worsening muscle regeneration and fibrosis vs. results from control

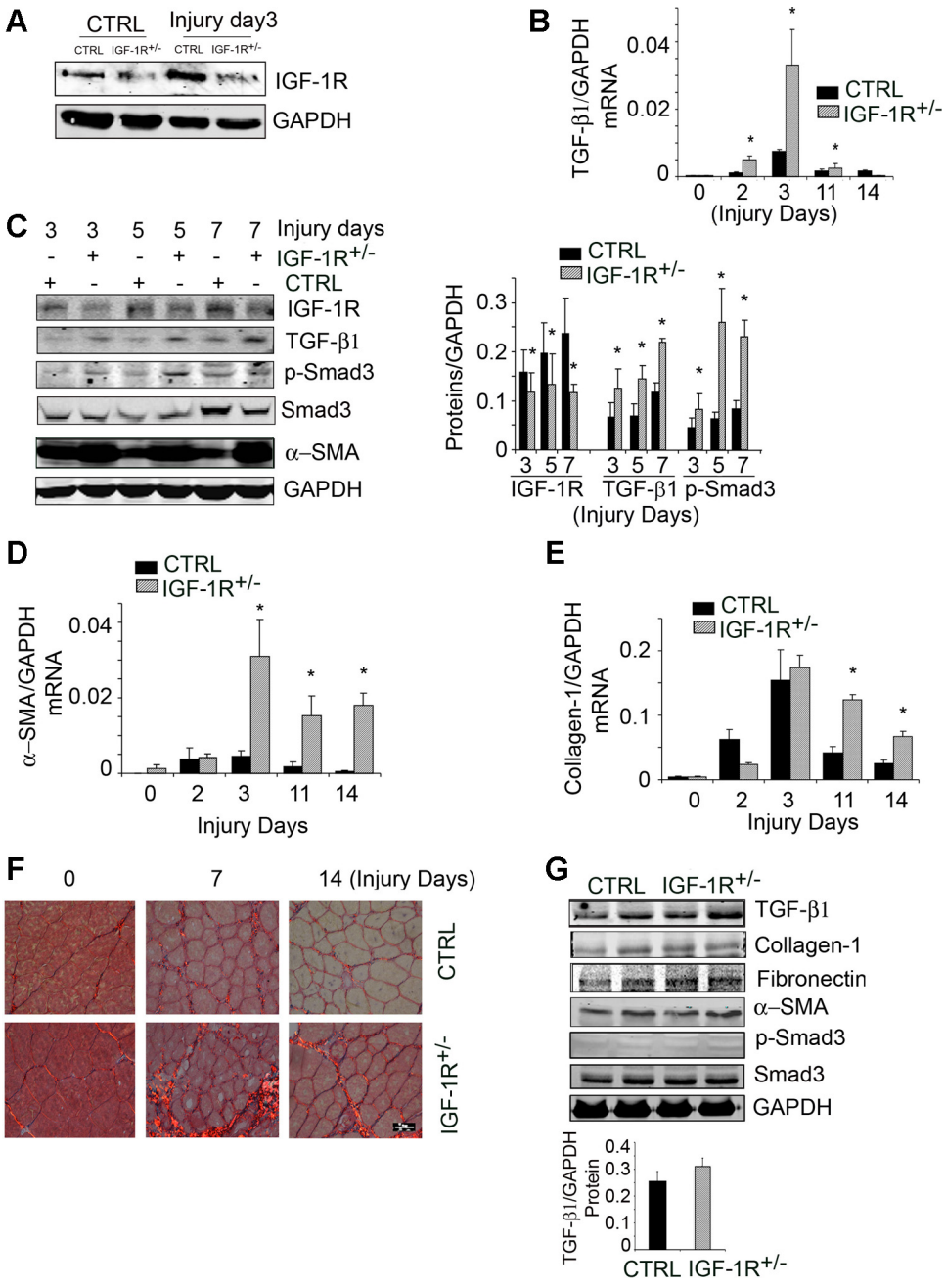

Fig. 4. IGF-IR$^{+/-}$ increases fibrosis in injured muscle. *A*: representative Western blots of IGF-IR from lysates of TA muscles 3 days after injury ($n = 4$ mice in each group). *B*: mRNA expression of TGF-β1 in injured TA muscles of CRTL and IGF-IR$^{+/-}$ mice ($*P < 0.05$ vs. values of control mice at different times; $n = 4$ mice at each time). *C*, *left*: representative Western blots of proteins in lysates of injured TA muscles; *right*: the density of bands representing different genes are corrected for GAPDH ($*P < 0.05$ vs. CTRL; $n = 4$ mice at each group). *D* and *E*: mRNAs of α-smooth muscle actin (α-SMA; *D*) and collagen I (*E*) in injured TA muscles of control and IGF-IR$^{+/-}$ mice ($*P < 0.05$ vs. CTRL; $n = 4$ mice in each group). *F*: cross-sections of TA muscles obtained at 7 or 14 days after injury were stained with Sirius red. The yellow-red color indicates collagen I deposition (bar, 50 μm; $n = 4$ mice in each group). *G*, *top*: representative Western blots of proteins in uninjured muscles of control and IGF-IR$^{+/-}$ mice at 12 wk of age ($n = 6$ control or IGF-IR$^{+/-}$ mice); *bottom*: the density of TGF-β1 bands is corrected for GAPDH ($n = 4$ mice at each group).

mice. Interestingly, the magnitude of decrease in the expression of myogenin in muscles of IGF-IR$^{+/-}$ mice was less than the decrease in IGF-IR, p-Akt, or MyoD. This presumably represents differing responses of genes that control satellite cell functions. For example, in mutant mice lacking both *Myf5* and *MyoD*, skeletal muscle was not formed (31), but in mice lacking myogenin, myoblasts were unaffected, but muscle fibers were scarce (14, 26).

We also noticed that muscle weight and total body weight had similar reductions in IGF-IR$^{+/-}$ mice, and this could be due to the fact that skeletal muscle (plus fat) constitutes ~60–80% of body weight in rats (30) and ~40–45% in humans, and therefore, loss of muscle will decrease total body weight. In addition, we found that satellite cells isolated from muscle of IGF-IR$^{+/-}$ mice had significantly reduced expression of IGF-IR and p-Akt as well as MyoD and myogenin, but the expression of the IGF-IR in satellite cells was lower than the IGF-IR level we detected in muscles of IGF-IR$^{+/-}$ mice. This difference could represent the total level of IGF-IR from muscle, blood vessels, and interstitial tissues as well as satellite cells compared with the results of isolated satellite cells.

An interaction between IGF-I and TGF-β1 signaling has been reported. In epithelial or hematopoietic cells it was shown that Akt interacts with Smad3, but the roles of Akt and p-Akt are controversial. In one report, p-Akt did not promote an interaction with Smad3, but in another report it was concluded that p-Akt is required for the inhibition of

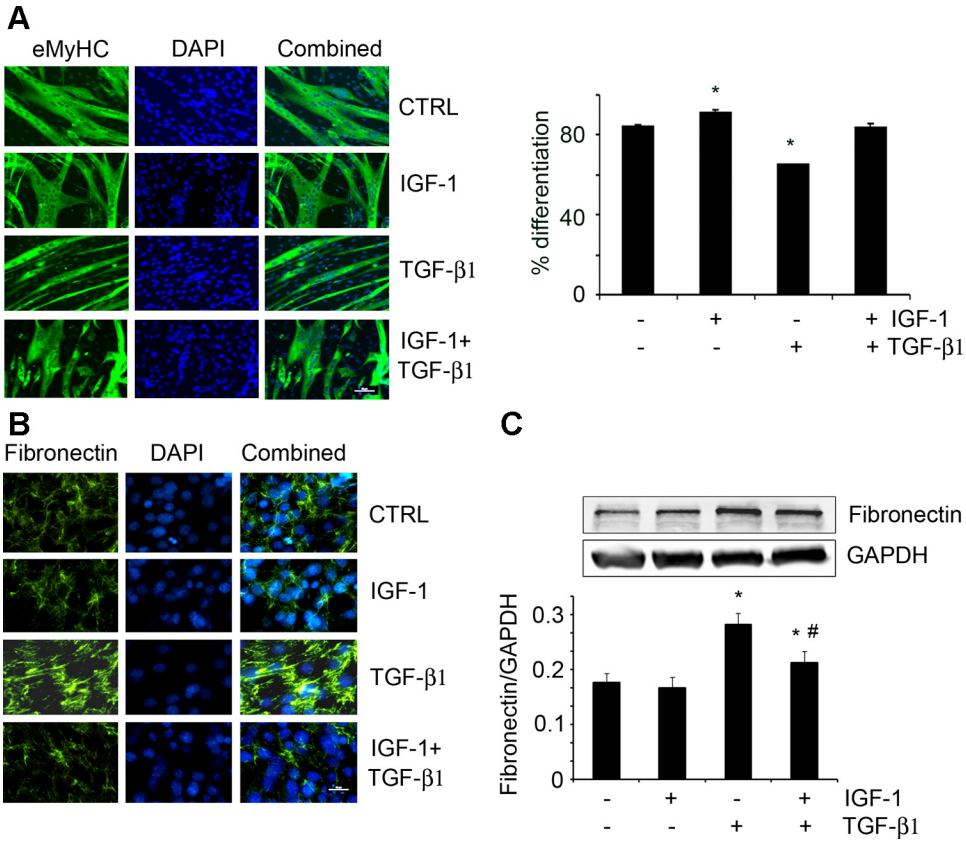

Fig. 5. IGF-I suppresses TGF-β1-induced fibrosis. *A*, *right*: C_2C_{12} cells were differentiated in media with IGF-I, TGF-β1, or both for 96 h and then immunostained with anti-eMyHC; *left*: the differentiation index (MATERIALS AND METHODS) was calculated; $n = 3$ repeats, $P <$ 0.05 vs. untreated cells. *B*: C_2C_{12} cells were treated with IGF-I, TGF-β1, or both for 8 h, and cells were immunostained with fibronectin (green; bar, 50 μm; $n = 3$ repeats). *C*: representative Western blots for fibronectin in C_2C_{12} cells treated with IGF-I, TGF-β1, or both for 8 h ($n = 3$ repeats). $*P < 0.05$ vs. nontreated cells; $\#P < 0.05$ vs. TGF-β1-treated cells.

Smad3 phosphorylation (8, 28). Our results indicate that both Akt and p-Akt are associated with Smad3 in mouse muscle and C_2C_{12} myoblasts. However, it appears that p-Akt is the major mediator regulating nuclear translocation of Smad3. Also, we found that a decrease in p-Akt in satellite cells isolated from IGF-IR$^{+/-}$ mice led to an increase in Smad3 translocation into nuclei. When C_2C_{12} cells were treated with IGF-I, p-Akt increased in the cytoplasm and was associated with Smad3, preventing Smad3 from mediating TGF-β1 signaling.

Satellite cell heterogeneity has been widely investigated, and it has been shown that both human and porcine satellite cells can differentiate into mature adipocytes (10, 36). Others conclude that individual satellite cells and their progeny can adopt only a single developmental fate (35), and Starkey et al. (39) concluded that satellite cells are committed to myogenesis and do not spontaneously adopt nonmyogenic fates. To explain why "satellite cells" isolated from IGF-IR$^{+/-}$ mice produce more TGF-β1 vs. satellite cells from control mice, two possibilities exists: *1*) isolated satellite cells could be a mix of two types of cells, muscle progenitor cells and cells with fibrogenic potential (19); or *2*) satellite cells respond to impaired IGF signaling by developing into fibroblast cells through a TGF-β1-stimulated pathway. Regardless, our report shows for the first time that IGF-I and TGF-β1 signaling are interacting in mouse satellite cells, determining the fate of satellite cells to either myogenesis or fibrogenesis.

There is evidence that Smad3 exerts an antimyogenic effect by a mechanism that depends on transcriptional repression of MyoD plus an inhibition of satellite cell differentiation into myotubes (21, 32). For example, in the mdx mouse, inhibition of p-Smad3 with halofuginone was shown to suppress muscle fibrosis and improve skeletal muscle function (18, 29, 41). In agreement with these conclusions that p-Smad3 interferes with myogenesis, we found that treatment with TGF-β1 increases translocation of Smad3 into nuclei and suppresses myoblast differentiation into myotubes (Fig. 5*A*) that may be responsible for worsening fibrosis.

In our experiments, we chose to study Smad3 rather than Smad2 because targeted knockdown of Smad2 in cultured human myoblasts only modestly reduced the ability of TGF-β1 to impair myotube formation. In contrast, loss of Smad3 or knockdown of Smad2 and Smad3 together was shown to sharply increase myotube formation (40). Similarly, Smad3 knockout has been shown to exert a major change in the differentiation into myotubes that occurs when cells were treated with TGF-β1; in those experiments, Smad2 KO resulted in only a small response (21, 22, 33).

Taken together, our results demonstrate that stimulation of IGF-IR signaling not only blocks TGF-β1-induced fibrosis in muscle but may also interrupt TGF-β1 signaling. This results in prevention of activation of Smad3 and its translocation into nuclei, where it increases mediators of fibrosis. Thus, the association of p-Akt with Smad3 in the cytoplasm in muscle or satellite cells provides a novel mechanism by which myogensis occurs and prevents fibrosis. Therefore, therapeutic strategies to enhance this association may prove beneficial in muscle injury.

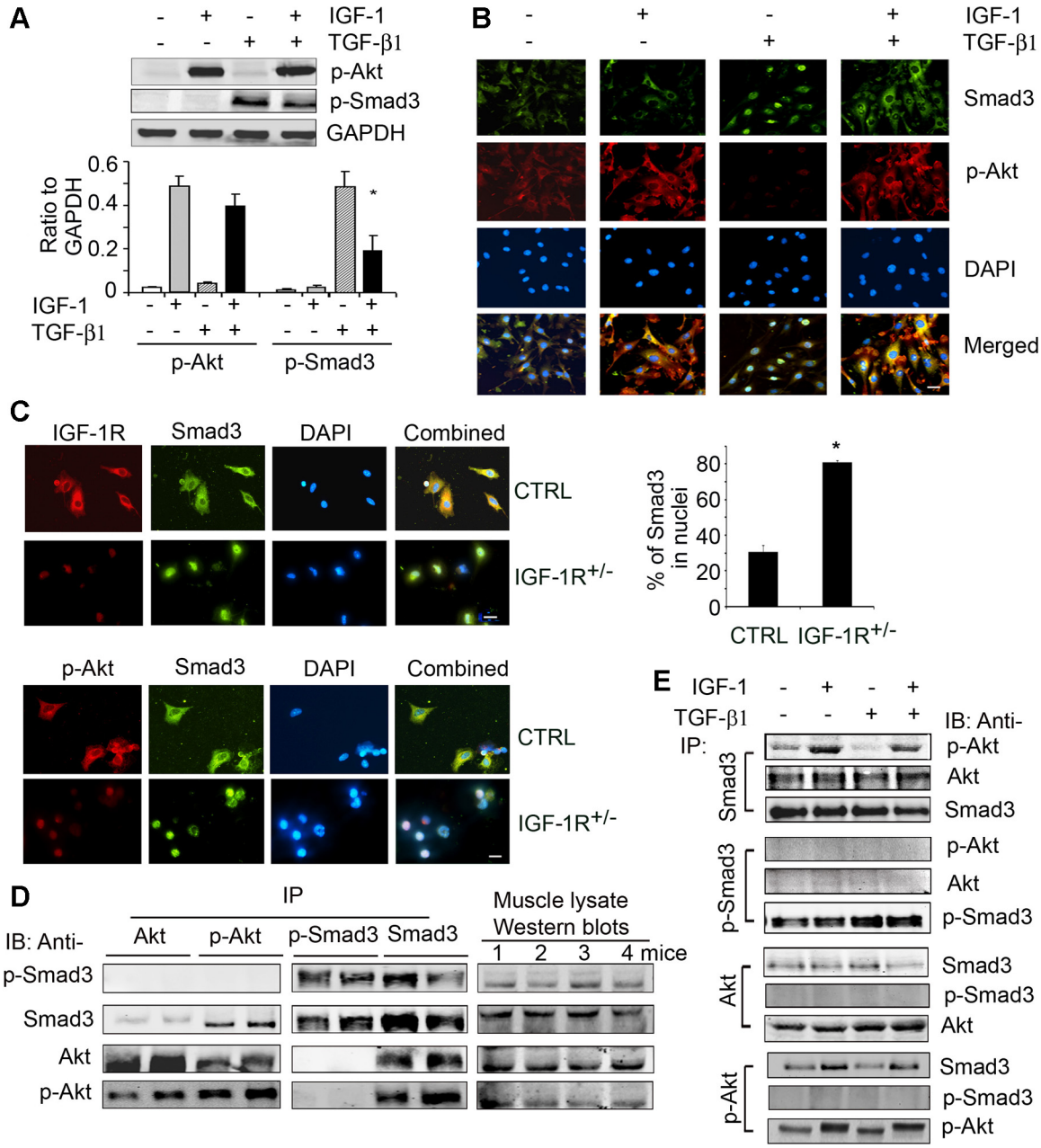

Fig. 6. p-Akt interacts with Smad3. *A*, *top*: representative Western blots of p-Akt and p-Smad3 in C_2C_{12} cells that were treated with IGF-I, TGF-β1, or both for 30 min; *bottom*: band densities corrected for GAPDH (*$P < 0.05$ vs. TGF-β1 treatment; $n = 3$ repeats). *B*: C_2C_{12} cells were treated with IGF-I, TGF-β1 or both for 15 min and then immunostained for Smad3 (Green) and p-Akt (red). Bar, 50 μm with 3 repeats. *C*, *left*: satellite cells from muscles of control or IGF-IR$^{+/-}$ mice were immunostained for Smad3 (green), IGF-IR, or p-Akt (red); *right*: the average of percentage of Smad3 in the nucleus was calculated from 10 fields (*$P < 0.05$ vs. CTRL, 3 repeats; bar, 50 μm). *D*: gastrocnemius muscle lysates from wild-type mice were immunoprecipitated with 4 different antibodies (anti-Smad3, anti-p-Smad3, anti-p-Akt, or anti-Akt), and each immunocomplex was subjected to Western blotting using antibodies to Smad3, p-Smad3, Akt, or p-Akt [$n = 3$ mice with immunoprecipitation (IP) and Western blotting repeated twice]. *E*: C_2C_{12} cells were treated with IGF-I, TGF-β1, or both for 30 min, cell lysates were immunoprecipited with antibodies recognizing Smad3, p-Smad3, Akt, or p-Akt, and then the imunocomplexes of each were subjected to Western blots with Smad3, p-Smad3, Akt, or p-Akt ($n = 4$ repeats).

ACKNOWLEDGMENTS

We thank Dr. William E. Mitch for critical review of the manuscript and Dr. and Mrs. Harold Selzman and Norman S. Coplo for their generous support.

GRANTS

This work was supported by extramural research grants from Satellite Health and the American Diabetes Association (1-11-BS-194) to L. Zhang and by National Institute of Diabetes and Digestive and Kidney Diseases Grants R37-DK-37175 and T32-DK-62706.

DISCLOSURES

No conflicts of interest, financial or otherwise, are declared by the authors.

AUTHOR CONTRIBUTIONS

Yanjun Dong, R.L., X.H.W., and L.Z. contributed to the conception and design of the research; Yanjun Dong, R.L., S.T., Yanlan Dong, K.A.S.S., and L.Z. performed the experiments; Yanjun Dong, R.L., and L.Z. analyzed the data; Yanjun Dong and L.Z. interpreted the results of the experiments; Yanjun Dong, R.L., and L.Z. prepared the figures; Yanjun Dong, R.L., and L.Z. drafted

the manuscript; Yanjun Dong, S.T., X.H.W., K.A.S.S., and L.Z. edited and revised the manuscript; Yanjun Dong, R.L., S.T., Yanlan Dong, X.H.W., K.A.S.S., and L.Z. approved the final version of the manuscript.

REFERENCES

1. **Allen RE, Boxhorn LK.** Inhibition of skeletal muscle satellite cell differentiation by transforming growth factor-beta. *J Cell Physiol* 133: 567–572, 1987.
2. **Anderson JE, Mitchell CM, McGeachie JK, Grounds MD.** The time course of basic fibroblast growth factor expression in crush-injured skeletal muscles of SJL/J and BALB/c mice. *Exp Cell Res* 216: 325–334, 1995.
3. **Barton ER, Morris L, Musaro A, Rosenthal N, Sweeney HL.** Muscle-specific expression of insulin-like growth factor 1 counters muscle decline in mdx mice. *J Cell Biol* 157: 137–147, 2002.
4. **Brack AS, Conboy MJ, Roy S, Lee M, Kuo CJ, Keller C, Rando TA.** Increased Wnt signaling during aging alters muscle stem cell fate and increases fibrosis. *Science* 317: 807–810, 2007.
5. **Chen JC, Mortimer J, Marley J, Goldhamer DJ.** MyoD-cre transgenic mice: a model for conditional mutagenesis and lineage tracing of skeletal muscle. *Genesis* 41: 116–121, 2005.
6. **Cheng J, Du J.** Mechanical stretch simulates proliferation of venous smooth muscle cells through activation of the insulin-like growth factor-1 receptor. *Arterioscler Thromb Vasc Biol* 27: 1744–1751, 2007.
7. **Conboy IM, Conboy MJ, Wagers AJ, Girma ER, Weissman IL, Rando TA.** Rejuvenation of aged progenitor cells by exposure to a young systemic environment. *Nature* 433: 760–764, 2005.
8. **Conery AR, Cao Y, Thompson EA, Townsend CM Jr, Ko TC, Luo K.** Akt interacts directly with Smad3 to regulate the sensitivity to TGF-beta induced apoptosis. *Nat Cell Biol* 6: 366–372, 2004.
9. **Couteaux R, Mira JC, d'Albis A.** Regeneration of muscles after cardiotoxin injury. I. Cytological aspects. *Biol Cell* 62: 171–182, 1988.
10. **De CP, Milan G, Scarda A, Boldrin L, Centobene C, Piccoli M, Pozzobon M, Pilon C, Pagano C, Gamba P, Vettor R.** Rosiglitazone modifies the adipogenic potential of human muscle satellite cells. *Diabetologia* 49: 1962–1973, 2006.
11. **Dobrowolny G, Giacinti C, Pelosi L, Nicoletti C, Winn N, Barberi L, Molinaro M, Rosenthal N, Musaro A.** Muscle expression of a local Igf-1 isoform protects motor neurons in an ALS mouse model. *J Cell Biol* 168: 193–199, 2005.
12. **Goldspink G, Fernandes K, Williams PE, Wells DJ.** Age-related changes in collagen gene expression in the muscles of mdx dystrophic and normal mice. *Neuromuscul Disord* 4: 183–191, 1994.
13. **Grounds MD.** Age-associated changes in the response of skeletal muscle cells to exercise and regeneration. *Ann NY Acad Sci* 854: 78–91, 1998.
14. **Hasty P, Bradley A, Morris JH, Edmondson DG, Venuti JM, Olson EN, Klein WH.** Muscle deficiency and neonatal death in mice with a targeted mutation in the myogenin gene. *Nature* 364: 501–506, 1993.
15. **Hawke TJ, Garry DJ.** Myogenic satellite cells: physiology to molecular biology. *J Appl Physiol* 91: 534–551, 2001.
16. **Holzenberger M, Leneuve P, Hamard G, Ducos B, Perin L, Binoux M, Le Bouc Y.** A targeted partial invalidation of the insulin-like growth factor I receptor gene in mice causes a postnatal growth deficit. *Endocrinology* 141: 2557–2566, 2000.
17. **Hu Z, Wang H, Lee IH, Modi S, Wang XH, Du J, Mitch WE.** PTEN inhibition improves muscle regeneration in mice fed a high fat diet. *Diabetes* 59: 1312–1320, 2010.
18. **Huebner KD, Jassal DS, Halevy O, Pines M, Anderson JE.** Functional resolution of fibrosis in mdx mouse dystrophic heart and skeletal muscle by halofuginone. *Am J Physiol Heart Circ Physiol* 294: H1550–H1561, 2008.
19. **Joe AW, Yi L, Natarajan A, Le GF, So L, Wang J, Rudnicki MA, Rossi FM.** Muscle injury activates resident fibro/adipogenic progenitors that facilitate myogenesis. *Nat Cell Biol* 12: 153–163, 2010.
20. **Li Y, Foster W, Deasy BM, Chan Y, Prisk V, Tang Y, Cummins J, Huard J.** Transforming growth factor-beta1 induces the differentiation of myogenic cells into fibrotic cells in injured skeletal muscle: a key event in muscle fibrogenesis. *Am J Pathol* 164: 1007–1019, 2004.
21. **Liu D, Black BL, Derynck R.** TGF-beta inhibits muscle differentiation through functional repression of myogenic transcription factors by Smad3. *Genes Dev* 15: 2950–2966, 2001.
22. **Liu D, Kang JS, Derynck R.** TGF-beta-activated Smad3 represses MEF2-dependent transcription in myogenic differentiation. *EMBO J* 23: 1557–1566, 2004.
23. **Mann CJ, Perdiguero E, Kharraz Y, Aguilar S, Pessina P, Serrano AL, Muñoz-Cánoves P.** Aberrant repair and fibrosis development in skeletal muscle. *Skelet Muscle* 1: 21, 2011.
24. **Miller KJ, Thaloor D, Matteson S, Pavlath GK.** Hepatocyte growth factor affects satellite cell activation and differentiation in regenerating skeletal muscle. *Am J Physiol Cell Physiol* 278: C174–C181, 2000.
25. **Musaro A, Giacinti C, Borsellino G, Dobrowolny G, Pelosi L, Cairns L, Ottolenghi S, Cossu G, Bernardi G, Battistini L, Molinaro M, Rosenthal N.** Stem cell-mediated muscle regeneration is enhanced by local isoform of insulin-like growth factor 1. *Proc Natl Acad Sci USA* 101: 1206–1210, 2004.
26. **Nabeshima Y, Hanaoka K, Hayasaka M, Esumi E, Li S, Nonaka I, Nabeshima Y.** Myogenin gene disruption results in perinatal lethality because of severe muscle defect. *Nature* 364: 532–535, 1993.
27. **Pelosi L, Giacinti C, Nardis C, Borsellino G, Rizzuto E, Nicoletti C, Wannenes F, Battistini L, Rosenthal N, Molinaro M, Musaro A.** Local expression of IGF-1 accelerates muscle regeneration by rapidly modulating inflammatory cytokines and chemokines. *FASEB J* 21: 1393–1402, 2007.
28. **Remy I, Montmarquette A, Michnick SW.** PKB/Akt modulates TGF-beta signalling through a direct interaction with Smad3. *Nat Cell Biol* 6: 358–365, 2004.
29. **Roffe S, Hagai Y, Pines M, Halevy O.** Halofuginone inhibits Smad3 phosphorylation via the PI3K/Akt and MAPK/ERK pathways in muscle cells: effect on myotube fusion. *Exp Cell Res* 316: 1061–1069, 2010.
30. **Ruderman NB, Houghton CR, Hems R.** Evaluation of the isolated perfused rat hindquarter for the study of muscle metabolism. *Biochem J* 124: 639–651, 1971.
31. **Rudnicki MA, Schnegelsberg PN, Stead RH, Braun T, Arnold HH, Jaenisch R.** MyoD or Myf-5 is required for the formation of skeletal muscle. *Cell* 75: 1351–1359, 1993.
32. **Sabourin LA, Girgis-Gabardo A, Seale P, Asakura A, Rudnicki MA.** Reduced differentiation potential of primary MyoD−/− myogenic cells derived from adult skeletal muscle. *J Cell Biol* 144: 631–643, 1999.
33. **Sartori R, Milan G, Patron M, Mammucari C, Blaauw B, Abraham R, Sandri M.** Smad2 and 3 transcription factors control muscle mass in adulthood. *Am J Physiol Cell Physiol* 296: C1248–C1257, 2009.
34. **Seale P, Sabourin LA, Girgis-Gabardo A, Mansouri A, Gruss P, Rudnicki MA.** Pax7 is required for the specification of myogenic satellite cells. *Cell* 102: 777–786, 2000.
35. **Shefer G, Wleklinski-Lee M, Yablonka-Reuveni Z.** Skeletal muscle satellite cells can spontaneously enter an alternative mesenchymal pathway. *J Cell Sci* 117: 5393–5404, 2004.
36. **Singh NK, Chae HS, Hwang IH, Yoo YM, Ahn CN, Lee SH, Lee HJ, Park HJ, Chung HY.** Transdifferentiation of porcine satellite cells to adipoblasts with ciglitizone. *J Anim Sci* 85: 1126–1135, 2007.
37. **Song K, Cornelius SC, Reiss M, Danielpour D.** Insulin-like growth factor-I inhibits transcriptional responses of transforming growth factor-beta by phosphatidylinositol 3-kinase/Akt-dependent suppression of the activation of Smad3 but not Smad2. *J Biol Chem* 278: 38342–38351, 2003.
38. **Song K, Wang H, Krebs TL, Danielpour D.** Novel roles of Akt and mTOR in suppressing TGF-beta/ALK5-mediated Smad3 activation. *EMBO J* 25: 58–69, 2006.
39. **Starkey JD, Yamamoto M, Yamamoto S, Goldhamer DJ.** Skeletal muscle satellite cells are committed to myogenesis and do not spontaneously adopt nonmyogenic fates. *J Histochem Cytochem* 59: 33–46, 2011.
40. **Trendelenburg AU, Meyer A, Rohner D, Boyle J, Hatakeyama S, Glass DJ.** Myostatin reduces Akt/TORC1/p70S6K signaling, inhibiting myoblast differentiation and myotube size. *Am J Physiol Cell Physiol* 296: C1258–C1270, 2009.
41. **Turgeman T, Hagai Y, Huebner K, Jassal DS, Anderson JE, Genin O, Nagler A, Halevy O, Pines M.** Prevention of muscle fibrosis and improvement in muscle performance in the mdx mouse by halofuginone. *Neuromuscul Disord* 18: 857–868, 2008.
42. **Tzanno-Martins C, Azevedo LS, Orii N, Futata E, Jorgetti V, Marcondes M, Duarte AJ.** The role of experimental chronic renal failure and aluminium intoxication in cellular immune response. *Nephrol Dial Transplant* 11: 474–480, 1996.
43. **Wang XH, Hu Z, Klein JD, Zhang L, Fang F, Mitch WE.** Decreased miR-29 suppresses myogenesis in CKD. *J Am Soc Nephrol* 22: 2068–2076, 2011.
44. **Zhang L, Dong Y, Dong Y, Cheng J, Du J.** Role of integrin-beta3 protein in macrophage polarization and regeneration of injured muscle. *J Biol Chem* 287: 6177–6186, 2012.
45. **Zhang L, Du J, Hu Z, Han G, Delafontaine P, Garcia G, Mitch WE.** IL-6 and serum amyloid A synergy mediates angiotensin II-induced muscle wasting. *J Am Soc Nephrol* 20: 604–612, 2009.
46. **Zhang L, Wang XH, Wang H, Hu Z, Du J, Mitch WE.** Satellite cell dysfunction and impaired IGF-1 signaling contribute to muscle atrophy in chronic kidney disease. *J Am Soc Nephrol* 21: 419–427, 2010.